DEM Simulations of the Progressive Collapse of Framed Structures

E. Masoero[1], F.K.Wittel[2], H.J. Herrmann[2], B.M. Chiaia[1]
[1]Politecnico di Torino, Torino, Italy; [2]Swiss Federal Institute of Technology, Zurich, Switzerland

Progressive collapse of framed structures is a complex topic going beyond the usual tools of structural mechanics. The analogy with the propagation of damage in the framework of fracture mechanics has already brought some theoretical results, especially when the energy fluxes are analyzed. Nevertheless, the difficulty to get representative experimental data avoids proposing and eventually proving the effectiveness of new theories modeling collapsing frames with equivalent homogeneous cracking continua (or foams). Therefore, reliable computer simulations based on widely accepted methods are necessary. Since traditional FEM are inapplicable when a structure looses rigidity, DEM have been used to run the simulations shown throughout this paper. The advantages, the limits and the problems of this approach are discussed and particular attention is paid to the effects of impacts between falling elements and the structural members.

1 INTRODUCTION

Local damage in buildings can occur due to accidental events like gas explosions, vehicle impact, gross design-construction errors or malicious terrorist attacks [1]. However, it can also be thoroughly planned as part of a controlled demolition processes with blast. We talk of progressive collapse if the damage, initiated by the loss of one or a few supporting elements, spreads in a chain like reaction. Its main characteristic is a final damage being strongly disproportionate to its original cause.

Progressive collapse of buildings received great attention having been promoted by outstanding catastrophic collapses. First interest in the subject rose after the partial collapse of Ronan Point apartments in London 1968, caused by a gas explosion. In the following years, the fundamental approaches to structural robustness where formulated. Lately, terrorist attacks e.g. against the Murrah Federal Building, Oklahoma City 1995, and the World Trade Center (WTC), New York 2001, renewed interest in the problem of progressive collapse and vulnerability of structures [2]. Today most design codes require tough structural elements to prevent local damage and redundancy to sustain it (Alternate Path Method, APM). Nevertheless, the fulfillment of the prescriptions of the codes is not always sufficient to prevent progressive collapse. For example [4] discussed the ineffectiveness of horizontal ties in thin steel ceilings or [5] showed the small ductility demand related to progressive collapse of 2D framed steel structures. Therefore advanced simulations are necessary in order to better understand the phenomena and mechanisms of progressive collapse of structures.

Progressive collapse is a dynamic phenomenon. Hence, models have to capture the dynamic nature of the process. As an example, the one-dimensional (1D) collapse of the WTC in a collapse model by [6, 7, 8] was given by the upper portion of the structure falling with an increasing mass onto the still intact lower one pro-

ducing progressive buckling of the columns. A closer look on the complicated geometry of a 2D framed structure however reveals diverse local rupture modes, e.g. buckling, shear, bending, tensile, crushing failures etc, and impact between falling elements and intact portions of the structure. Such collapse can only be captured by computer simulations. Refs. [9, 10, 11] point out the importance of dynamics even in the first stages of the collapse, when the structure responds to the sudden loss of a supporting element in contrast to a static APM analysis. Only few simulations capture the whole process with the impact between falling rubble and still intact portions of the structure. In refs. [12,13] special beam Finite Element (FE) macro-elements are developed that are able to consider the impacts of masses. In such FE macro-element based models each structural element is represented by one beam or plate element. They are numerically advantageous but their application to more realistic 3D frames is complicated by catenary effects of ceilings that are often neglected for this cause [14], and by the many possible scenarios of impact between the falling elements. In contrast, in FE micro-element models every structural element is finely meshed. This way catenary effects of the ceilings and impacts between the structural elements and with the ground can be considered [15, 16]. Unfortunately this is numerically expensive, prohibiting extensive parametric studies.

We propose an alternative approach via Discrete Element Methods (DEM). We study the response of 3D framed structures after the removal of one column. We show that DEM are a suitable approach, since the mechanical response, as well as the inter-particle contacts are captured within a robust and efficient simulation scheme, allowing for parametric studies. The importance of impacts in the transition from partial to total collapse is pointed out and the local mechanisms driving the damage propagation are discussed. The energetics of the collapse and resulting fragment size distributions are studied in detail. The paper is organized as follows: First we describe the method, model parameters and simulation method used throughout the paper, before we study the collapse simulations first from a macroscopic and later from a mechanistic point of view. We complete the paper with conclusions and an outlook.

2 SIMULATING PROGRESSIVE COLLAPSE

The progressive collapse of framed structures shows complex dynamics, including sectional ruptures of beams and columns, formation of fracture lines in the ceiling slabs, multiple buckling and impacts of falling elements with still standing portions of the structure and with the ground, just to name a few. For this study DEM is used for several reasons [17]. First of all, DEM is naturally suitable for dynamic problems since it is based on the direct integration of Newton's equations of motion, leading to simple and fast algorithms. Furthermore geometrical and mechanical nonlinearities like large displacements and local ruptures can be easily modeled without remeshing. Finally, momentum transmissions due to contacts between structural elements can be included straightforwardly (see Sec. 2.2). Disadvantages are the need for a rather fine mesh to reduce the discretisation errors for the volume representation and discrete local fracture (see Sec. 2.2) and small time increments that come along with the hard body contact of stiff ele-

ments. First we will discuss the geometric parameterization of the frame structure, then the discretisation and material in the DEM framework, before we discuss details of the simulation.

2.1 Model Construction

The study is focused on geometries of simple flat slab structures consisting of a regular 3D frame of $4 \times 4 \times 4$ identical square cuboid cells with edge lengths L, and H (see Fig. 1; Table 1). The structure consists of columns in Z direction, clamped to the ground (Z = 0m) and connected at each story by principal beams in X and Y direction. Thin slabs spanning between the principal beams constitute the ceilings while vertical walls are neglected.

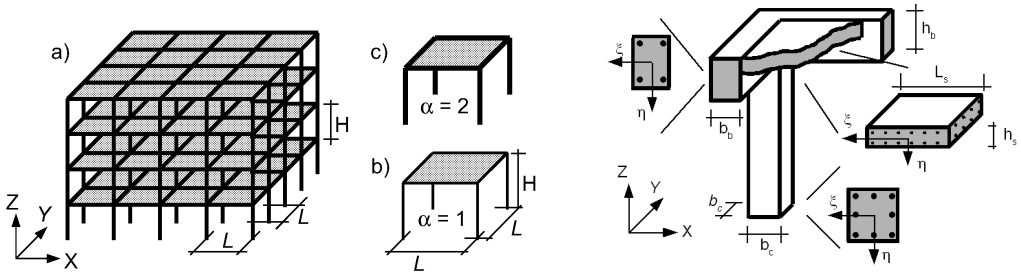

Fig. 1: The studied frame structure and elementary cells with b) $\alpha = 1$ and c) $\alpha = 2$. and cross sections of structural elements and disposition of the reinforcement. Subscripts *c*, *b* and *s* used for column, beam and slab.

The structure is thought to be made of reinforced concrete (RC) with Young's modulus E and Poisson's ratio ν. Geometrical quantities of the element's cross sections are given in (Fig. 1). We define their heights proportional to their length using the coefficients λ_c, λ_b and λ_s scaled with a uniform dimensionless geometry parameter α. Note that larger α enlarges element cross sections, leading to stiffer and stronger structures. The aspect ratio of beam and column cross sections is defined by the coefficients δ_b and δ_c. Resulting cross sectional areas A, inertias I with respect to the principal axes and torsion inertias are summarized in Table 1. Note that ceiling slabs are subdivided into square cuboid portions $L_s \times L_s \times h_s$ (Fig. 1); Sec. 2.2) with L_s independent on α.

2.2 Model Description

The structure is idealized with Euler-Bernoulli (EB) beam elements [19] connecting nodes. A sphere is centered on each node (Fig. 2.b) to avoid penetration of nodes. They also represent the volume occupied by the surrounding material. Columns and beams are represented by 8 EB beam elements, while ceilings are subdivided in 8×8 slabs portions (Fig. 1) whose centers of mass are placed on a plane square grid of EB beam elements (Fig. 2.a). The cross sections of the beam elements are set according to Sec. 2.1. Since the horizontal displacements due to bending are negligible compared to the vertical ones, we assumed $I_\eta = I_\xi$.

Parameter		*Unit*	*Value*
Bay of the cell	L	m	4
Height of the cell	H	m	3
Columns slenderness	λ_c	–	1/9
Beams slenderness	λ_b	–	1/8.5
Slabs slenderness	λ_s	–	1/50
Columns sec asr	δ_c	–	1
Beams sec asr	δ_b	–	2/3
Slabs portion sec asr	δ_s	–	$\lambda_s L/L_s$ $= 8/50$
Columns tc	$f(\delta_c)$	–	0.141
Beams tc	$f(\delta_b)$	–	0.196
Slabs portion tc	$f(\delta_s)$	–	0.264
Columns steel-RC ar	$\rho_{s,c}$	–	0.0145
Beams steel-RC ar	$\rho_{s,b}$	–	0.0109
Slabs portion steel-RC ar	$\rho_{s,s}$	–	0.0198
RC Young modulus	E	N/m^2	$30{\cdot}10^9$
RC Poisson ratio	ν	–	0
RC specific weight	γ_{RC}	kg/m^3	2500
Steel Young modulus	E_s	N/m^2	$210{\cdot}10^9$
Steel yield axial strain	ϵ_y	–	0.00178
Columns sec area	A_c	m^2	$\delta_c\alpha^2\lambda_c^2H^2$
Beams sec area	A_b	m^2	$\delta_b\alpha^2\lambda_b^2L^2$
Slabs portion sec area	A_s	m^2	$\alpha\lambda_s LL_s$
Columns sec inertia ξ and η	$I_{\xi,c}, I_{\eta,c}$	m^4	$1/(12\delta_c)A_c^2$
Beams sec inertia ξ and η	$I_{\xi,b}$,$I_{\eta,b}$	m^4	$1/(12\delta_b)A_b^2$
Slab portion sec inertia ξ and η	$I_{\xi,s}$,$I_{\eta,s}$	m^4	$1/(12L_s^2)A_s^3$
Columns sec torsion inertia	$I_{t,c}$	m^4	$f(\delta_c)/\delta_cA_c^2$
Beams sec torsion inertia	$I_{t,b}$	m^4	$f(\delta_b)/\delta_bA_b^2$
Slabs port. sec tors. inertia	I_tt,s	m^4	$f(\delta_s)/L_s^2A_s^2$

Parameter		*Unit*	*Value*
Dead load	G_d	kg/m^2	285
Live load	Q	N/m^2	660
Gravity acceleration	g	m/s^2	10
Mesh of the columns	L_c	m	0.375
Mesh of the beams	L_b	m	0.5
Mesh of the ceiling slabs	L_s	m	0.5
Columns tensile th	$\epsilon_{max,c}$	‰	$\rho_{s,c}E^* = 0.18$
Beams tensile th	$\epsilon_{max,b}$	‰	$\rho_{s,b}E^* = 0.14$
Slabs portion tensile th	$\epsilon_{max,s}$	‰	$\rho_{s,s}E^* = 0.25$
Columns rot th	$\Theta_{max,c}$	rad	$3\epsilon_{max,c}0.9\alpha\lambda_c \cdot HL_c/(8I_{\xi,c})$
Beams rot th	$\Theta_{max,b}$	rad	$\epsilon_{max,b}A_b0.9\alpha\lambda_b \cdot LL_b/(2I_{\xi,b})$
Slabs portion rot th	$\Theta_{max,s}$	rad	$\epsilon_{max,s}A_s^20.9/(2I_{\xi,s})$
Beam damping coef.	$\gamma_{l,Q,M}$	kg/s	0.06
Columns spheres ∅	D_c	m	$0.95L_c = 0.35625$
Beams/slabs portion spheres ∅	D_b,D_s	m	$0.95L_{b,s}$
Spheres overlapping stiffness	Y	N/m^2	10^6
Spheres normal and tangent dc	γ_n,γ_t	kg/s	10000
Spheres friction coef.	μ	–	0.3
Ground overlapping stiffness	Y^G	N/m^2	10^8
Ground normal and tangent dc	γ_n^G,γ_t^G	kg/s	10^5
Ground friction coef.	μ^G	–	10^5
Pre-dumping duration	t_d	s	$0.1 - 0.3$
Simulation end	t_e	s	8.1

threshold (th); coefficient (coef); dissipation coefficient (dc); area ratio (ar); aspect ratio (asr); sectional (sec); rotation (rot); torsional constant (tc); E*=E,ε,/E

Table 1: Model and simulation parameters.

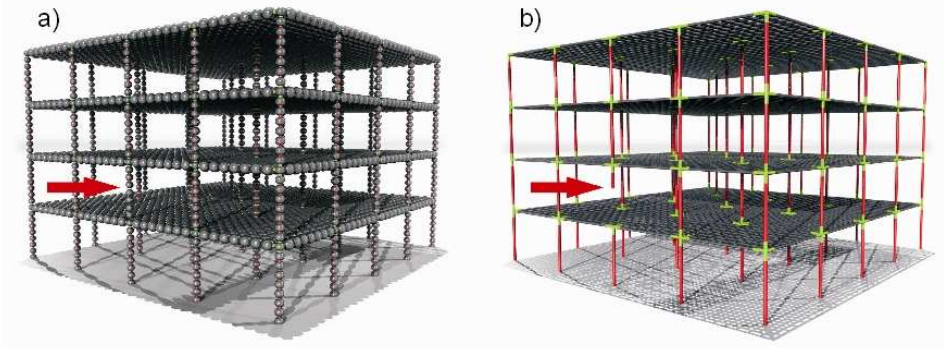

Fig. 2: Discretized structure with a total amount of 9248 EB beam elements (a) and 5081 spheres (b). The arrow points at the element where damage is initiated.

The mass M_i of a generic sphere i is obtained by adding an extra mass $M_{EX,i}$, for the dead load to the sum of half the masses $M_{EB,j}$ of the m EB elements attached to the node, namely

$$M_i = M_{EX,i} + \sum_{j=1}^{m} \frac{1}{2} M_{EB,j}. \qquad (1)$$

Therefore the masses of the EB elements are eventually concentrated in the nodes, while the sphere's rotation inertia is calculated with uniformly distributed mass. Every node is subjected to the gravity force and an external force for the live load

on all horizontal beams and ceilings. If beams are connected to it, three moments and forces transmitted via the beams themselves are added as well [19].
The generic beam connecting node *i* and node *j* can fail according to the breaking rule $\varepsilon/\varepsilon_{\max} + \Theta/\Theta_{\max} \geq 1$, with the axial strain ε and the elongation threshold ε_{max}. Θ denotes the maximum bending at the nodes divided by EI/L_{ij}, with *I* momentum of inertia of the cross section and initial beam length L_{ij} and Θ_{max} the corresponding rotational threshold. In detail,

$$\Theta = \max\left\{\left|4\varphi_{\xi,i} + 2\varphi_{\xi,j}\right|, \left|2\varphi_{\xi,i} + 4\varphi_{\xi,j}\right|, \left|4\varphi_{\eta,i} + 2\varphi_{\eta,j}\right|, \left|2\varphi_{\eta,i} + 4\varphi_{\eta,j}\right|\right\}, \quad (3)$$

with rotation $\varphi_{\xi,i}$ with respect to the ξ axis of the cross section at node *i*, referring to the line connecting node *i* to node *j*. The adopted criterion neglects failures under pure compression, assuming perfectly brittle coupled axial and bending failure without plastic stress redistributions in this stage of the model. The failure thresholds are calculated starting from the uncoupled ultimate pure axial force $N_{th} = A_s \varepsilon_y E_s$, and the ultimate plastic moment $M_{th} = A_{s,\inf} \varepsilon_y E_s 0.9h$ around the ξ axis of the cross section, where only the strength contribution of the steel (Fig. 3) at its yield point is considered. A_s is the area of reinforcement in the cross section, $A_{s,inf}$ is the inferior portion of A_s, *h* denotes the height of the cross section and 0.9 is a coefficient that relates *h* to the distance between the inferior and the superior reinforcement. Since the RC section with the geometrical and mechanical parameters in Table1 should break at N_{th} and M_{th} in uncoupled strain state, the equivalent full-reacting section failure thresholds come out to be

$$\varepsilon_{th} = \frac{N_{th}}{AE} = \rho_s \frac{E_s \varepsilon_y}{E}, \qquad \Theta_{th} = \frac{M_{th} L_{ij}}{EI_\xi}. \quad (5)$$

Internal damping of beams is taken into account through the coefficients in Table 1. If two spheres overlap, a contact force, calculated by a Hertzian contact law with high elastic modulus and damping coefficients is added to the respective nodes. If a sphere touches the ground an additional contact is considered [17]. For simplicity, disorder in breaking thresholds or geometries is neglected.

2.3 Numerical Method and Simulations

To follow the time evolution of the system, the explicit time integration of the Newton's equations of motion is calculated via a 5th order Gear-Predictor-Corrector algorithm [18]. The time increment used throughout the simulation decreases with α because the stiffness of the system grows. The element geometry, high stiffness of building materials and overlapping moduli, lead to time steps in the order of 10^{-5}-10^{-6}s. Nevertheless, we have to simulate the long duration process (2-8s) of collapse which is the principal limitation for the size of the systems that can be simulated.
The simulations start in the undeformed configuration and the structures are instantaneously loaded by gravity and live loads. The subsequent deformations generate a state of strain and stress in the beam elements that tends to balance the external load. In this simulation stage, we overdamp the system by setting the velocities of all the nodes to zero as soon as the overall kinetic energy reaches a maximum, until the equilibrium is reached. Subsequently an accidental event is

simulated by the removal of an external column (Fig. 2), leading to elastic dynamic stress redistribution. Consequently other beam elements can become overstressed and fail. Ruptures can disconnect whole portions of the structure from the rest that impact against intact ones. The simulations stop 8 real-time seconds after the accidental event.

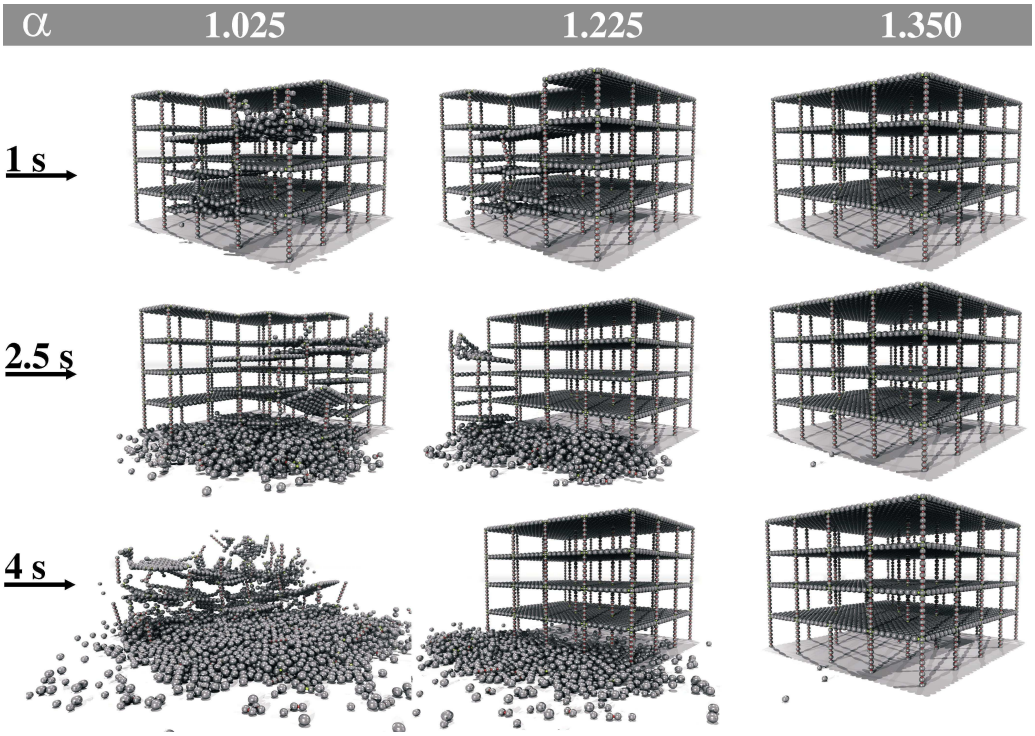

Fig. 3: Collapse evolution for structures with increasing α.Simulation parameters are summarized in Tab. 1.

3 PROGRESSIVE COLLAPSE OF FRAMED STRUCTURES

We perform simulations of various systems that only differ by a single geometry parameter α described in Sec. 2.1. By changing α, we simulate robust structures, partially collapsing and fully destroyed ones. Snapshots of the system are given in Fig. 3 for three values of α. First we report on overall properties like system energies, damage evolution, degree of structural collapse or fragment distribution of rubble, before we address local failure mechanisms of the collapse in Sec. 4.

3.1 Energetics

The evolution of different energies in the system are important to confirm the analysis. Note that energy can only be dissipated by the formation of damage and due to damping when particles collide. If the stress redistribution induced by the initial damage is sufficient to disconnect a portion of the structure, the average kinetic energy $\langle E_K \rangle$ starts to grow almost quadratically in time due to the free fall. Then, the impact of falling slabs on still intact ones underneath them as well as with the ground produces bumps in the $\langle E_K \rangle$ plot (Fig. 4.a). (Fig. 4.b) shows the growth of the number of broken bonds in time.

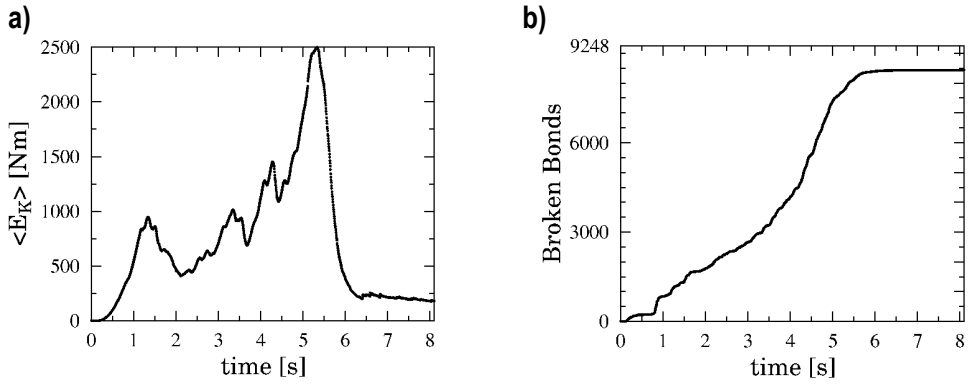

Fig. 4: Time evolution of the kinetic energy and the number of broken bonds during the collapse for $\alpha = 1.125$.

3.2 Transitions in the final stage of the collapse

The damage evolution in terms of broken bonds is not sufficient to characterize the degree, a structure has collapsed. Therefore we define the *survival space* in the structure as the ratio between the structural volume V_S that is still standing and serviceable and the initial volume V. Its dual is the *demolition rate DR*, defined as $DR=(V-V_S)/V$.

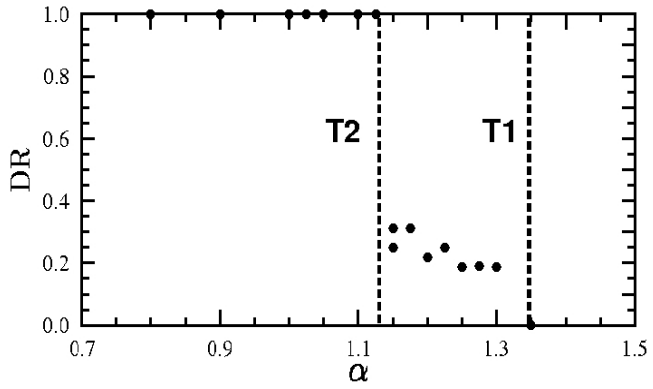

Fig. 5: Demolition rate as function of α.

The DR – α plot (Fig. 5) shows two transitions: T1 from partial to no collapse ($\alpha = 1.35$) and T2 from total to partial collapse ($\alpha = 1.125$). T1 is exclusively produced by dynamic elastic stress redistribution and therefore could be evidenced through classical approaches neglecting the impacts. Differently, T2 is definitely impact-dependent and is a novel result of the proposed approach. T2 is very important for the design of robust structures ($\alpha > 1.35$). A partial collapse could be acceptable in the prospective of an optimization involving a minimization of costs and negative consequences of the collapse. In this context, the *DR* jump from the 20-30% of the partial collapse regime and the 100% of the total collapse regime can make the difference between a robust and a vulnerable response of a reasonably economic structure.

3.3 Scaling behavior of rubble

A quantitative characterization of the final collapse for systems with varying α is possible by analysing the composition of the rubble in terms of fragment masses. Therefore a cluster analysis is performed and resulting cumulative fragment mass distributions are shown in (Fig. 6.a). Partially collapsed ($1.125<\alpha<1.35$) and fully collapsed ($\alpha<1.125$) structures are clearly separated in two distinct regimes.

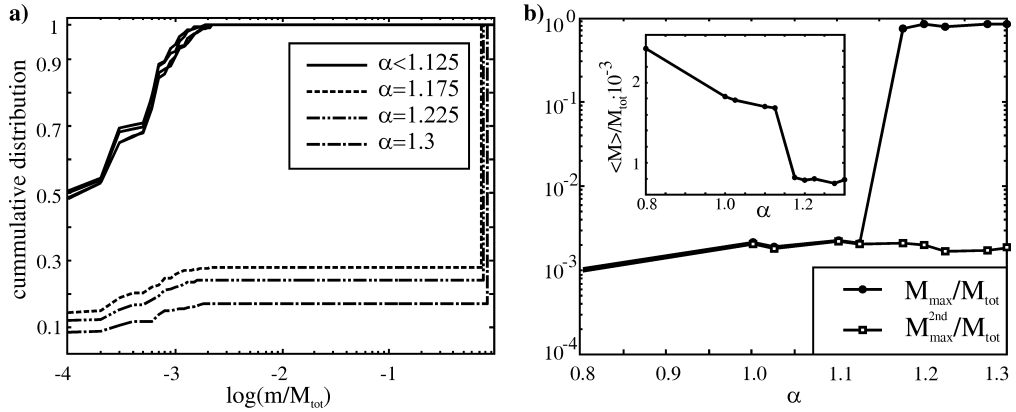

Fig. 6. Fragment mass distribution and analysis of the rubble.

For demolition purposes the size of the largest and second largest fragment is of interest. They prove to be not very sensitive to α (see Fig. 6.b) when normalized by the total mass of the system. In this plot, partial collapse is characterized by a sudden difference between the largest and second largest fragment for $\alpha \approx 1.15$. In the inset the normalized average fragment mass decreases with increasing α, meaning a better degree of fragmentation. The reason in believed to be the higher impact energy of structural parts, since their weight increases with α.

4 MECHANISMS OF COLLAPSE

During the different stages of the progressive collapse, several mechanisms of the damage propagation can be observed, depending on α and time. Some of them are not visible in classical collapse simulations and in fact also not in our model if we omit inter-particle or particle-ground contacts. The first collapse stage is dominated by the elastic dynamic stress redistribution after the damage initiation. The second collapse stage is dominated by inter-particle contacts and three distinct mechanisms can be defined, namely the hammer effects, drag and base cutting mechanisms (see Fig. 7).

- The hammer effect arises from impacts between the falling ceilings and the still intact ones underneath them. The large sudden transmission of energy generally fragments the underlying ceiling and can induce rupture of the columns of neighboring structural cells.
- The damage propagation due to drag originates from lateral impacts between falling rubble and still intact portions of the structure. The impact can break the beams and columns of neighboring cells and trigger further collapses. This mechanism shows the strongest sensitivity to modeling details like the starting conditions.

- The base cutting mechanism is triggered by rubble that piles up on the ground exerting lateral pressure on the base columns of the still intact portions of the structure. The eventual loss of one of these base columns goes along with large stress redistributions and elastic waves that can trigger a large propagation of the further collapse.

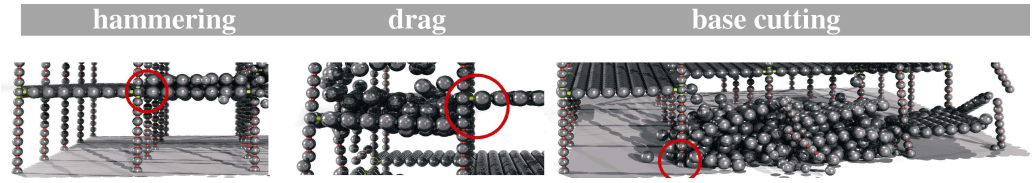

Fig. 7: Observed local mechanisms leading to collapse.

Interestingly, when we switch off all contacts it turns out, that elastic dynamic redistributions aren't able to induce a complete collapse in well designed structures (i.e. structures that are able to carry the service load without failures when not damaged by a starting accidental event). Furthermore, neglecting the presence of the ground, which is equal to switching off the column base cutting mechanism, moves the transition point between total and partial collapse from $\alpha = 1.125$ to $\alpha = 1$. This means that in the region $1<\alpha<1.125$ hammer and drag mechanisms alone are not sufficient for complete collapse. However, the exact numerical values might be effected by the low degree of redundancy in our structure and the lack of vertical walls and material plasticity.

5 CONCLUSIONS AND OUTLOOK

We presented a simulation study on the progressive collapse of parameterized flat slab structures, following elastic dynamic stress redistribution due to the loss of one structural element. By changing the geometric control parameter α, we go from robust structures to partially and completely collapsed ones, exhibiting a complex sequence of damage propagation mechanisms. It was demonstrated, that calculations with purely dynamic load redistribution without the possibility for rubble impacts are not sufficient to provoke more than partial collapse. The relevance of the hammering effect suggests that targeted attacks on base columns could be less hazardous than those aimed at upper ones. In the first case the kinetic energy of the falling ceilings will be transmitted to the ground and only part of it will be available for base cutting of neighboring columns. Of course, this conclusion must be validated also for the case when crushing collapse of the columns due to stress redistributions is admitted, since in this case the loss of a base column could be much more critical. Moreover, the loss of a base column provokes a more energetic initial dynamic stress redistribution that increases the probability that farther portions of the structure can fail and trigger an impact-driven catastrophic progressive collapse. Including disorder into the mechanical properties of the elements as well as geometrical imperfections will probably bring more detailed and realistic results concerning the fragment size distribution. Taking into account the possibility for plastic stress redistributions and a higher degree of redundancy e.g. by internal walls, would affect the collapse scenario towards more robustness. The goal of such optimization should be the prevention

of complete collapse. Works to include plasticity and refined failure criteria that also account for column crushing and eccentric compression ruptures that distinguish between steel and concrete are in progress.

REFERENCES

[1] M. Levy, M. Salvadori, Why Buildings Fall Down?, Norton, New York, 1992

[2] D.V. Val, E.G. Val, Robustness of framed structures, Struct Eng Int 16(2) (2006) 108-112

[3] R.S. Nair, Progressive collapse basics, Mod Steel Constr 44(3) (2004) 37-44

[4] A.G. Vlassis, B.A. Izzudin, A.Y. Elghazouli, D.A. Nethercot, Design oriented approach for progressive collapse assessment of steel framed buildings, Structu Eng Int 16(2) (2006) 129-136

[5] K. Khandelwal, S. El-Tawil, S.K. Kunnath, H.S. Lew, Macromodel-based simulation of progressive collapse: steel frame structure, J Struct Eng – ASCE 134(7) (2008) 1070-1078

[6] Z.P. Bažant, M. Verdure, Mechanics of the progressive collapse: learning from the World Trade Center and building demolition, J Eng Mech – ASCE 133(3) (2007) 308-319

[7] G.P. Cherepanov, I.E. Esparragoza, Progressive collapse of towers: the resistance effect, Int J Fract 143 (2007) 203-206

[8] K.A. Seffen, Progressice collapse of the World Trade Center, J Eng Mech – ASCE 134(2) (2008) 125-132

[9] G. Kaewkulchai, E.B. Williamson, Dynamic behavior of planar frames during progressive collapse, Proceedings of the 16th ASCE Engineering Mechanics Conference, Seattle, July 16-18, 2003

[10]] S. Marjanishvili, E. Agnew, Comparison of various procedure for progressive collapse analysis, J Perform Constr Fac 20(4) (2006) 365-374

[11] A.J. Pretlove, M. Ramsden, A.G. Atkins, Dynamic effects in progressive failure of structures, Int J Impact Eng 111(4) (1991) 539-546

[12] G. Kaewkulchai, E.B. Williamson, Beam element formulation and solution procedure for dynamic progressive collapse and analysis, Comp & Struct 82(7-8) (2004) 639-651

[13] D.E. Grierson, L. Xu, Y. Liu, Progressive-failure analysis of buildings subjected to abnormal loading, Comput Aided Civ Inf 20 (2005) 155-171

[14] D. Isobe, M. Tsuda, Seismic collapse analysis of reinforced concrete framed structures using the finite element method, Earthq Eng Struct D 32(13) (2003) 2027-2046

[15] D. Hartmann, M. Breidt, et al, Structural collapse simulation under consideration of uncertainty, Comput Struct in press

[16] B.M. Luccioni, R.D. Ambrosiani, R.F. Danesi, Analysis of building collapse under blast load, End Struct 26 (2004) 63-71

[17] T. Pöschel, T. Schwager, Computational Granular Dynamics, Springer 2005

[18] M.P. Allen, D.J. Tildesley. Computer Simulation of Liquids. Oxford Pr, 1987

[19] H.A. Carmona, F.K. Wittel, F. Kun, H.J. Herrmann: Fragmentation processes in impact of spheres, Phys Rev E 77 (2008) 051302